# Sensitivity Investigation of Substrate Thickness and Reflow Profile on Wafer Level Film Failures in 3D Chip Scale Packages by Finite Element Modeling

Bin Xie[1], Xunqing Shi[2]*, and Xuejun Fan[3]
[1]Advanced Electronic Manufacturing Center, Shanghai Jiao Tong University, Shanghai 200030, P. R. China
[2]Flash Manufacturing Group, Intel Technology Development (Shanghai) Ltd., Shanghai 200131, P. R. China
[3]Q&R Assembly Technology Development, Intel Corporation, 5000 W Chandler Blvd., Chandler, AZ 85226
*Email: daniel.shi@intel.com Phone: +86-21-38733114 Fax: +86-21-50481212

**Abstract**

3D chip scale package (CSP) is one of the major trends in IC packaging with the application of wafer level films (WLF) for die-to-die or die-to-substrate attachment. However, the WLF failures (voiding/cracking) are often observed in moisture sensitivity test. Substrate thickness and reflow profile were found very sensitive to the WLF failure rate. To investigate the sensitivity of the substrate thickness and the reflow profile, a novel direct concentration approach (DCA) is developed in this study, which allows updating the interfacial continuous condition as the function of the temperature and humidity. The paper also develops a simplified micromechanics-based vapor pressure model to visualize the whole-field vapor pressure corresponding to the instantaneous moisture distribution. With the applications of the DCA and the simplified vapor pressure model to a 3D ultra-thin stacked-die CSP, it was found that the moisture transport and escape during the reflow is the root cause of the WLF failures. A small reduction of the substrate thickness and an in-situ baking during the reflow can reduce greatly the moisture concentration and the vapor pressure at the bottom film, and therefore significantly decrease the WLF failure rate.

## Introduction

3D chip scale package (CSP) is one of the major trends in IC packaging. Wafer level films (WLF) has been widely used for die-to-die or die-to-substrate attachment because of its compactness, reliability and process simplicity. However, The WLF failures (voiding/cracking) were often found after the moisture sensitivity test, in which the soaking and the reflow processes are involved. The WLF failures jeopardize the package reliability by the current leakage or electrical open due to the displacement and deformation of the metallization layer. They also provide the paths for the moisture ingression to cause the interconnection corrosion, which deteriorates the device reliability performance.

Many experiments were performed to investigate the failure mechanism of WLF voiding/cracking. The substrate thickness and the reflow profile were found very sensitive to the voiding/cracking behavior and the WLF failure rate [1-3]. Small change of the substrate thickness could induce the significant difference of the failure rate. Different failure rate occurred after the reflow process with the different reflow profiles, though all the reflow profiles meet the JEDEC standard. Fundamental understanding of the sensitivity of the substrate thickness and the reflow profile on the WLF voiding/cracking is therefore necessary.

Moisture is believed to play an important role for the WLF failures. To investigate the sensitivity of the substrate thickness and the reflow profile, the understanding of the moisture redistribution and transportation in the CSP during the reflow is essential. The existing normalization approaches are efficient to develop the moisture diffusion modeling in the soaking process at the constant ambient temperature and humidity conditions [4, 5]. However, such approaches can not be applied to perform the moisture diffusion modeling during the reflow process at varying ambient temperature and humidity conditions, because the solubility and the saturated moisture concentration of materials change with the temperature and time.

The moisture is vaporized during the reflow and as a result the large vapor pressure is generated, which is the dominant driving force for the WLF failures. The knowledge of the vapor pressure evolution is the key to understand the failure mechanism due to the moisture vaporization. One way to obtain the vapor pressure distribution and evolution is the vapor pressure modeling. Many vapor pressure models were reported to implement the vapor pressure modeling, such as the micromechanics-based model [6-14]. The micromechanics-based model is widely used because it links to the intrinsic moisture property of the material and indicates more straightforward vapor pressure physics in the microscopic level.

This paper presents a novel direct concentration approach (DCA), which can allow updating interfacial continuous condition as the function of the temperature and humidity. This paper also develops a simplified micromechanics-based vapor pressure model to derive the vapor pressure distribution and evolution as a function of the temperature, time and local moisture concentration. Based on the above development of the moisture diffusion and vapor pressure modeling, the sensitivity of the substrate thickness and the reflow profile in the 3D ultra-thin stacked-die CSP is investigated. The competing effects between the temperature rise and the local moisture concentration drop on the non-monotonic evolution of the vapor pressure during the reflow are discussed. The design guidelines for optimizing the substrate dimensions and the reflow profile are provided.

## Direct Concentration Approach—Moisture Diffusion with Varying Ambient Temperature and Humidity

Moisture concentration is discontinuous across the material interface, when the two materials which have the

different saturated concentration $C_{sat}$ are jointed [4]. The interfacial discontinuity can be removed by normalizing the field variable. Galloway *et al.* developed an approach called partial pressure approach [4] with a new variable $\varphi$, which is defined by

$$\varphi = C / S \tag{1}$$

where $\varphi$ is the partial pressure, $C$ is the moisture concentration and $S$ is the solubility. The solubility $S$ is the material property and the function of the temperature.

This normalization approach is efficient to perform the moisture diffusion modeling during the soaking at the constant ambient temperature and humidity conditions, with the governing differential equation using the thermal-moisture analogy methodology

$$\frac{\partial^2 \varphi}{\partial x^2} + \frac{\partial^2 \varphi}{\partial y^2} + \frac{\partial^2 \varphi}{\partial z^2} = \frac{1}{D}\frac{\partial \varphi}{\partial t} \tag{2}$$

and the interfacial continuity

$$C^{(1)} / S_1 = C^{(2)} / S_2 \tag{3}$$

where *x, y, z* are coordinates, $D$ is the moisture diffusivity, $t$ is the time, $C^{(1)}$ is the moisture concentration at the interface on the material 1 (Mat1) side, $C^{(2)}$ is the moisture concentration at the interface on the material 2 (Mat2) side, $S_1$ and $S_2$ are the solubility of the Mat1 and Mat2 respectively.

Wong *et al.* [5] introduced the wetness fraction approach with an alternative variable $w$ (wetness), which is defined as

$$w = C / C_{sat} \tag{4}$$

The $w$ is also continuous at the interface because the saturated moisture concentration $C_{sat}$ is related to the solubility $S$ by

$$S = C_{sat} / p_{ext} \tag{5}$$

where $p_{ext}$ is the ambient vapor pressure at the given thermal and humid conditions. The wetness fraction approach is also efficient to perform the moisture diffusion modeling during the soaking.

However, when the temperature $T$ varies with the time $t$, the solubility $S$ as a function of the temperature $T$ becomes dependent on the time $t$. The governing differential equation becomes

$$\frac{\partial^2 \varphi}{\partial x^2} + \frac{\partial^2 \varphi}{\partial y^2} + \frac{\partial^2 \varphi}{\partial z^2} = \frac{1}{D}\frac{\partial \varphi}{\partial t} + \frac{\varphi}{D \cdot S}\frac{\partial S}{\partial t} \tag{6}$$

in which

$$\frac{\varphi}{D \cdot S}\frac{\partial S}{\partial t} \neq 0 \tag{7}$$

The similar issue occurs in the wetness fraction approach. This implies that the normalization approaches can not be used to develop the moisture diffusion modeling correctly even for a homogeneous material when the ambient temperature and humidity vary (such as reflow process), if using the typical governing differential equation with the thermal-moisture analogy methodology.

In order to accurately perform the moisture diffusion modeling with the varying temperature and humidity, a direct concentration approach (so-called DCA) is introduced in this paper. Different from the normalization approaches, the moisture concentration $C$ is directly used as the basic field variable, which is always continuous in each bulk of materials. Therefore, the typical governing differential equation can still be used, but the solubility $D$ is dependent on the temperature $T$ and the time $t$, which is given by

$$\frac{\partial^2 C}{\partial x^2} + \frac{\partial^2 C}{\partial y^2} + \frac{\partial^2 C}{\partial z^2} = \frac{1}{D(t)}\frac{\partial C}{\partial t} \tag{8}$$

However, $C$ is discontinuous at the material interface. Additional treatment is necessary to ensure the following interfacial continuous conditions

$$C^{(1)} / S_1(t) = C^{(2)} / S_2(t) \tag{9}$$

$$D_1(t)\frac{\partial C^{(1)}}{\partial n} = D_2(t)\frac{\partial C^{(2)}}{\partial n} \tag{10}$$

where $D_1(t)$ and $D_2(t)$ are the moisture diffusivity of the Mat1 and Mat2 respectively, and $n$ is the normal direction of the location at the interface. Eq. (10) is the requirement for the moisture flux continuity. The solubility and diffusivity of all the materials are the functions of the temperature $T$, and thus dependent on the time $t$.

**Simplified Micromechanics-based Vapor Pressure Model**

The DCA is introduced above to develop the moisture diffusion modeling with the varying temperature and humidity conditions in the macroscopic level. To estimate the vapor pressure in the porous spaces, where the moisture condenses into the mixed liquid-vapor phase or the single vapor phase, the vapor pressure model should be considered in the microscopic level. In the microscopic level, the attention is focused on what happens at a mathematical point, which is a representative elementary volume (REV) around any considered point in the porous medium domain [7]. The REV is defined in such a way that wherever it is placed within the considered porous medium domain, it always contains both the solid phase and the porous phase, and the moisture content in this representative volume is obtained as the moisture concentration from the moisture diffusion analysis in the macroscopic level. Furthermore, both the solid phase and the porous phase are assumed to be more or less evenly distributed within the REV. Therefore, the interstitial space fraction $f$ (or free volume fraction), which is considered as the intrinsic material property, can be introduced. Fan *et al.* [13] developed a micromechanics-based vapor pressure model, in which three distinct cases are identified to describe the moisture states in the pores. In the following, a vapor pressure model that greatly simplifies the original vapor pressure model [7] will be introduced, but the exact same results can be obtained. The new model to be presented does not need to relate the current moisture state to a reference moisture state.

The instantaneous moisture density $\rho$ in the pores is defined as [7]

$$\rho = C / f \tag{11}$$

When the moisture density $\rho$ is less than the saturated water vapor density $\rho_g$, the moisture is in the single vapor phase, and the vapor pressure can be calculated with the ideal gas law as follows

$$p(T) = \frac{RT}{MM_{H_2O} f} \cdot C \text{, when } C(T) / f < \rho_g(T) \tag{12}$$

where $R$ is the universal gas constant, $MM_{H_2O}$ is the molecular mass of water.

When the moisture density $\rho$ is more than the saturated vapor density $\rho_g$, the moisture in the pores is in the mixed liquid-vapor phase, and the vapor pressure stays as the saturated water vapor pressure as follows

$$p(T) = p_g(T), \quad \text{when} \quad C(T) / f \geq \rho_g(T) \tag{13}$$

where $p_g$ is the saturated water vapor pressure. Fig. 1 illustrates the two distinct moisture states in the pores, which can fully describe the instantaneous moisture states in the pores.

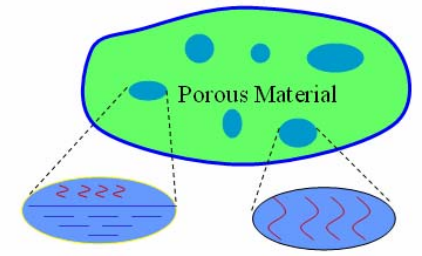


Fig. 1: Two distinct instantaneous states of the moisture in the porous material

**Numerical Implementation of Moisture Diffusion and Vapor Pressure Modeling**

Since the moisture diffusion modeling is considered at the conditions of the varying temperatures and humidity, the moisture field and the temperature field should be coupled. Although the duration of the reflow is short comparing with the duration of the soaking, the effect of the temperature field on the moisture diffusion and redistribution can not be neglected during the reflow. In order to perform the fully coupled thermal-moisture modeling, the "MASS DIFFUSION" analysis type is used in the commercial finite element analysis (FEA) software of ABAQUS for the moisture diffusion modeling. The adoption of this analysis type can guarantee Eq. (8) to be remained as the governing differential equation. The temperature field of the moisture diffusion modeling is obtained from the "HEAT TRANSFER" analysis type. All the material properties can be input as the functions of the temperature.

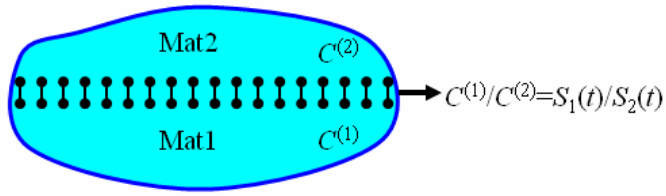


Fig. 2: Special treatment at the interface of the direct concentration approach

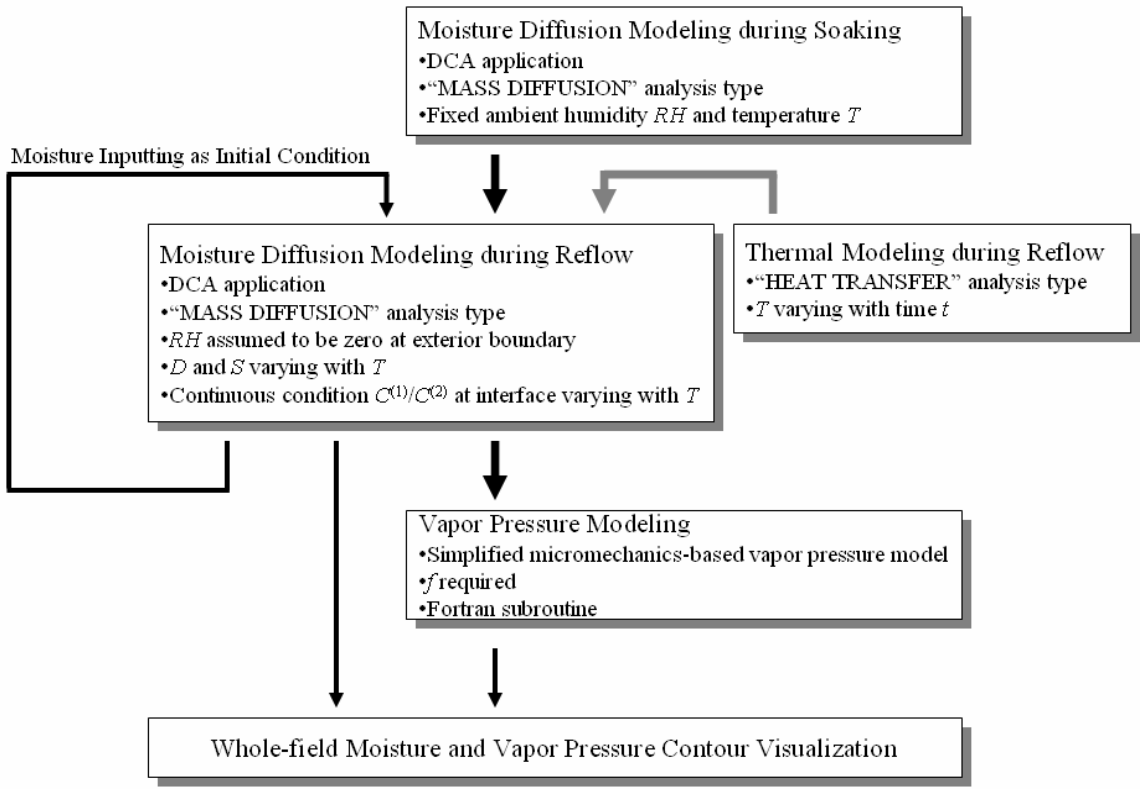


Fig. 3: Implemental procedure of the advanced modeling approaches for the moisture diffusion and vapor pressure

When the DCA is applied, the special treatment should be implemented to ensure the interfacial continuous conditions, as shown in Eqs. (9) and (10). Two separate sets of nodes are applied at the bi-material interface to represent the discontinuity of the moisture concentration, as shown in Fig. 2. The constraint equation or the multi-point constraint (MPC) is applied for each pair of nodes based on the Eq. (9) to join two materials together. The constraint equation is given by

$$C^{(1)} / C^{(2)} = S_1(t) / S_2(t) \quad (14)$$

According to the variational principle, Eq. (10) will be automatically satisfied through the finite element formulation procedure as long as the Eq. (9) is guaranteed.

Because the solubility of all the materials varies with the temperature and the time, the interfacial continuous equations also vary with the temperature and the time. However, most of the available commercial software does not allow automatically updating the constraint equation for the different steps. In order to update the interfacial continuous conditions, each time when the continuous conditions change, a new job should be submitted with the final moisture condition of the previous step as the initial moisture condition of the new step.

From the simplified vapor pressure model described above, the vapor pressure is also a whole-field distribution and is a simple transformation from the local moisture concentration as long as the interstitial space fraction $f$ is known. A FORTARN subroutine is written for ABAQUS to compute the value of vapor pressure and display the contour of vapor pressure at each increment. The contours of both the moisture distribution and the vapor pressure can therefore be output and visualized. Fig. 3 describes the whole implemental procedure of the moisture diffusion and vapor pressure modeling.

**Modeling Applications in the 3D Ultra-thin Stacked-die Chip Scale Package (CSP)**

The DCA and the simplified vapor pressure model can be applied to the various types of package. The 3D ultra-thin stacked-die CSP is adopted to study the distribution and evolution of the moisture and the vapor pressure in the package during the preconditioning and investigate the moisture-induced failure mechanism of WLF. The CSP composes molding compound (MC), silicon die, film, solder resist (SR) and BT core, as shown in Fig. 4. Half package is modeled due to the geometry symmetry. 2D model is adopted for the simplicity. Fig. 4 shows the shortened package with the typical structure. In the previous study, most WLF failures were found to occur in the bottom film. Therefore, the study of the failure mechanism focuses on the bottom film in this paper. The material properties used in this paper were measured by in-situ moisture absorption method and were detailed in Ref. [15].

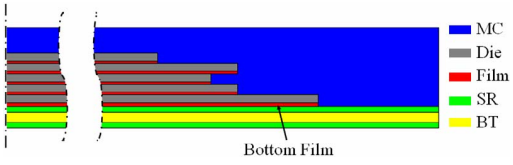


Fig. 4: The schematic structure of the 3D ultra-thin stacked-die chip scale package

*I. Effect of Substrate Thickness*

The substrate thickness was found sensitive on the failure rate of the bottom film. To investigate the sensitivity and achieve the failure-free in the package, advanced modeling approaches were applied to the packages with the thin substrate and the thick substrate. The contours of the moisture concentration with two different thickness substrates under the reflow profile1 at 260°C are shown in Fig. 5. The reflow profile1 is shown in Fig. 6. The moisture inside the MC and all the films except the bottom film with the thin substrate is similar as that with the thick substrate, while the moisture inside the bottom film with the thin substrate is much less than that with the thick substrate. A significant amount of moisture inside the bottom film is released through the substrate during the reflow. The moisture diffusion path with the thin substrate is shorter than that with the thick substrate, therefore more amount of the moisture was remained inside the bottom film of the package with thick substrate as compared to that with thin substrate. The moisture concentrations at the outmost point of the substrate/film interface are 0.71kg/m$^3$ and 1.55kg/m$^3$ respectively for the thin and thick substrate, as shown in Fig. 5. The moisture can be reduced by 118.31% during reflow for the thin substrate. Fig. 7 shows the whole moisture updating histories during the reflow process from 60°C to 260°C at the outmost point of the substrate/film interface for the thin and thick substrate. The moisture in the package with the thin substrate is always less than that with the thick substrate, and the largest moisture difference occurs around 230°C~250°C. The modeling results show that the substrate of the ultra-thin CSP is almost the only path for the moisture release during the reflow. It is totally different from the 'regular' packages with the much thicker substrate, in which the moisture release mainly occurs on the exterior of the packages and the moisture release in the die-attach film is negligible.

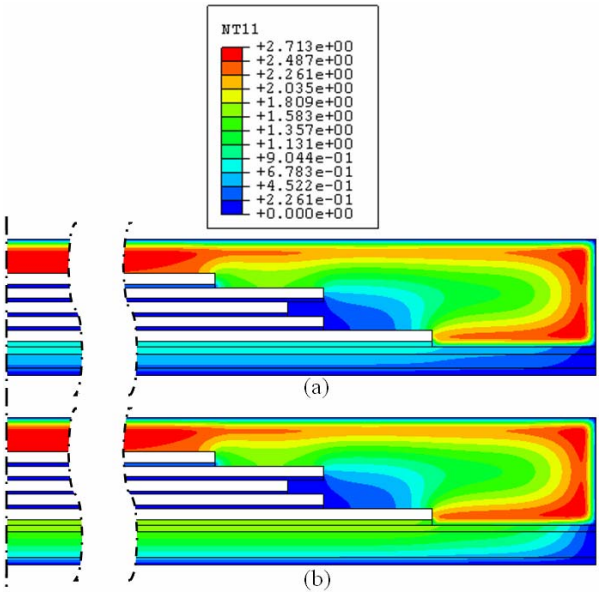


Fig. 5: Moisture contours at 260°C of the package with (a) the thin substrate and (b) the thick substrate

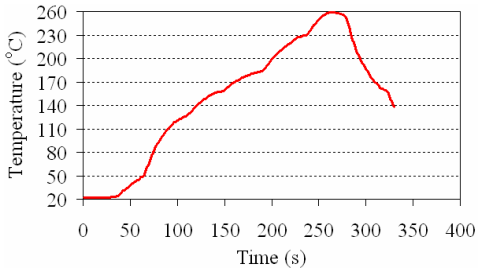


Fig. 6: Reflow profile1

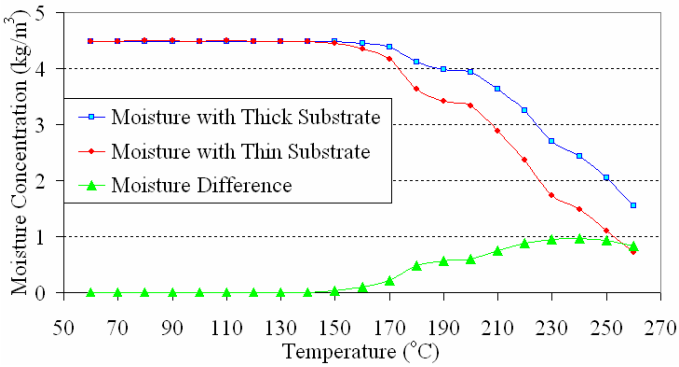


Fig. 7: Moisture comparison between the applications of the thin substrate and the thick substrate

The contours of vapor pressure at 260°C when $f$=0.05 for the thin and thick substrate are shown in Fig. 8. The vapor pressure inside the bottom film of the package with the thin substrate is much smaller than that with the thick substrate. The vapor pressures at the outmost point of the substrate/film interface for the thin and thick substrate under the reflow temperature of 260°C are 3.50MPa and 5.84MPa respectively. The vapor pressure can be reduced by 67.15% for the thin substrate. Fig. 9 shows the whole vapor pressure evolution histories during the reflow process from 60°C to 260°C at the outmost point of the substrate/film interface for two substrates. The vapor pressure of the package with the thick substrate is at the saturated level under the highest reflow temperature of 260°C, while the vapor pressure of the package with the thin substrate drops significantly. Around 260°C, the vapor pressure with the thick substrate reaches to the peak value of about 6MPa, which is large enough to cause the WLF failures with the small material strength at the high reflow temperature. At such high reflow temperature, the thermal stress due to the coefficient of thermal expansion (CTE) mismatch and the hygro-stress due to the polymer swelling are limited, because the elastic modulus of the WLF is less than 3MPa, and a 10% elastic strain only generates 0.3MPa stress. Therefore, the vapor pressure dominates the driving force, which causes the WLF failure at the high reflow temperature.

The comparisons of the vapor pressure difference and the moisture difference are shown in Fig. 10. It is noted that the largest moisture difference does not occur at 260°C, while the largest vapor pressure difference occurs at 260°C. The largest vapor pressure difference of about 2.4MPa is large enough to cause the different failure rate on the bottom film between the two substrates. Therefore, the application of the thin substrate can reduce the failure rate significantly or achieve the failure-free in the 3D ultra-thin stacked-die CSP.

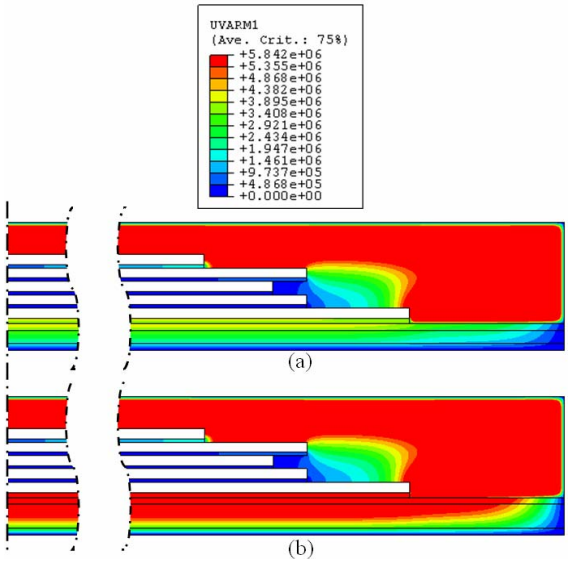


Fig. 8: Vapor pressure generated at the highest reflow temperature of 260°C for the packages with (a) the thin substrate and (b) the thick substrate

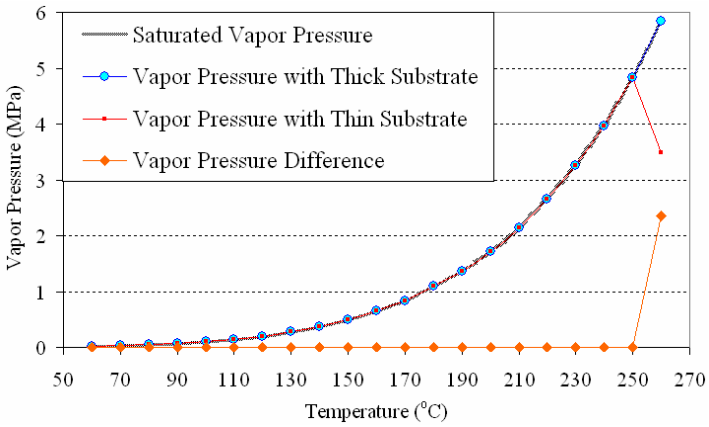


Fig. 9: Comparison on the vapor pressure during reflow process for the thin and thick substrate

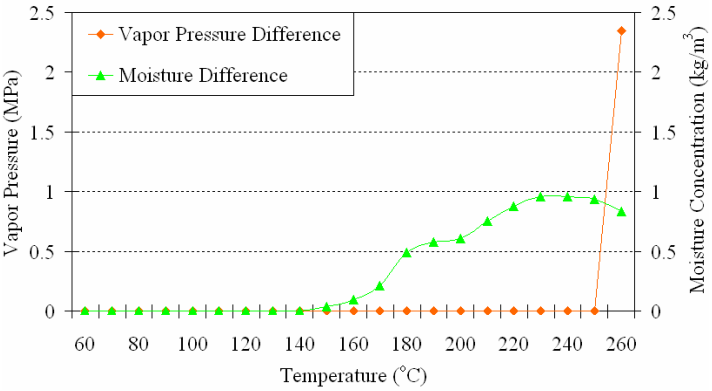


Fig. 10: Comparisons on the vapor pressure difference and moisture difference between the thin substrate and the thick substrate

*II. Effect of Reflow Profile*

Reflow profile was also found to have significant effect on the failure rate of the bottom film in the previous study. Fig. 11 shows the two different reflow profiles, both of which meet the JEDEC standard. The profile2 extends the ramp-up rate by adding a short time in-situ baking step comparing with the profile1. The contours of moisture concentration at 250°C with two reflow profiles are shown in Fig. 12. The moisture inside the MC and all the films except the bottom film with the profile2 is similar as that with the profile1, while the moisture inside the bottom film with the profile2 is less than that with the profile1, indicating that the in-situ baking can desorp more moisture through the substrate. The moisture concentrations at the outmost point of the substrate/film interface for the profile1 and profile2 are 1.11kg/m$^3$ and 0.73kg/m$^3$, respectively. The moisture can be reduced by 52.05% if using the reflow profile2.

The contours of vapor pressure at 250°C with $f$=0.05 under the profile1 and profile2 are shown in Fig. 13. The vapor pressures inside the MC and all the films except the bottom film are similar for the two profiles, while the vapor pressure inside the bottom film with the profile2 is much smaller than that with the profile1. The vapor pressures at the outmost point of the substrate/film interface for the profile1 and profile2 are 4.83MPa and 3.53MPa respectively. The vapor pressure can be reduced by 36.88% if using the reflow profile2.

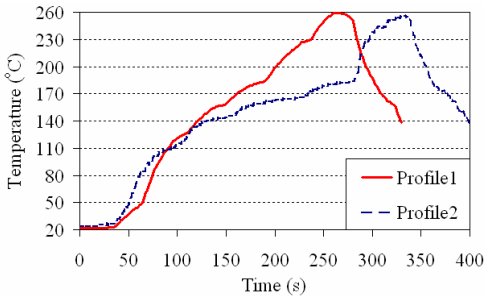


Fig. 11: Reflow profile1 and profile2

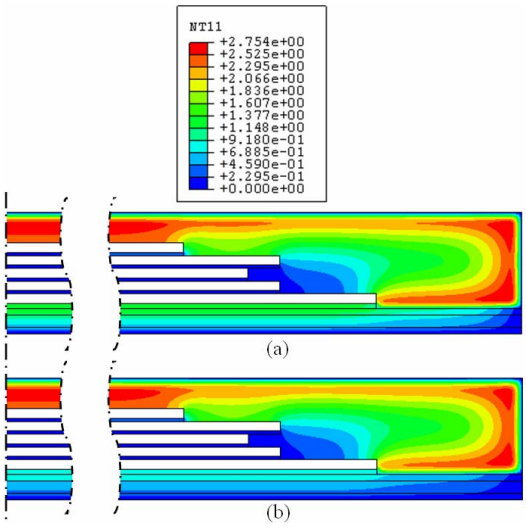


Fig. 12: Moisture contours at 250°C with the reflow (a) profile1 and (b) profile2

Fig. 14 shows the whole vapor pressure evolution histories during the reflow process from 60°C to 260°C at the outmost point of the substrate/film interface for two reflow profiles. The vapor pressures with two reflow profiles are remained at the saturated level during the most of reflow process, while large vapor pressure difference occurs at the high reflow temperatures. The largest vapor pressure difference is about 1.3MPa at 250°C, which is large enough to cause different failure rate on the bottom film between the two reflow profiles. Therefore, the application of the reflow profile with the in-situ baking can significantly reduce the failure rate of the bottom film.

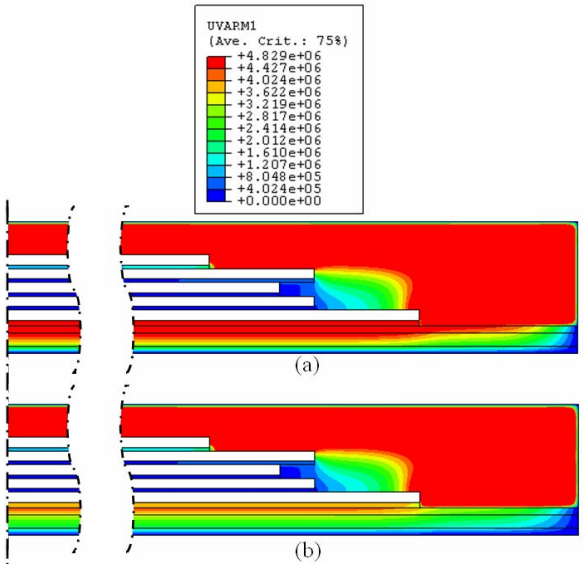


Fig. 13: Vapor pressure at 250°C with the reflow (a) profile1 and (b) profile2

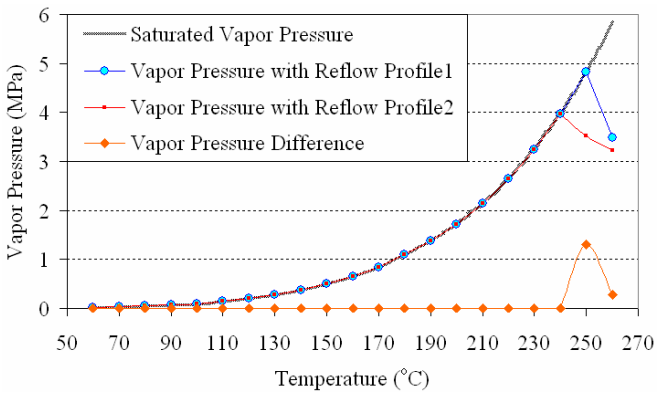


Fig. 14: Vapor pressure comparison between the reflow profile1 and profile2

**Conclusions**

Through the application of constraint equation at the material interface, the direct concentration approach (DCA) was developed to simulate the moisture diffusion at the conditions with varying ambient temperature and humidity. A simplified micromechanics-based vapor pressure model with the user-defined subroutine was established to determine the

whole-field vapor pressure corresponding to the instantaneous moisture distribution.

Based on the developed DCA and simplified vapor pressure model, the following conclusions can be reached:

A. The non-monotonic evolution of the vapor pressure because of the competing effects between the temperature rise and the local moisture concentration drop is responsible for the voiding/cracking of the WLF.

B. The vapor pressure is not always proportional to the local moisture concentration. The vapor pressure increases exponentially with the saturated vapor pressure when the moisture inside the pores is in the mixed liquid/vapor phase, while decreases gradually when the moisture inside the pores is in the single vapor phase. Moisture concentration has significant effect on the value of vapor pressure at high reflow temperature.

C. With the applications of the DCA and the simplified vapor pressure model to the 3D ultra-thin stacked-die CSP, the moisture transport and escape during the reflow is found to be the root cause of the bottom film failure. The substrate thickness and the reflow profile are sensitive to the failure rate of the bottom film. Applications of the thin substrate and the reflow profile with the in-situ baking can reduce the moisture concentration and the vapor pressure inside the bottom film significantly, and further reduce the failure rate and achieve the failure-free 3D ultra-thin stacked-die CSP.

**Acknowledgments**

The project was the collaboration between the Flash Manufacturing Group (FMG) Q&R, Shanghai and the Assembly Technology Development (ATD), Chandler, Arizona. We are thankful to the MIFFT (Moisture Induced Failure Focus Team) team members for stimulating discussions.

**References**

1. X. J. Fan, X. Q. Shi, İ. Bekâr, E. Prack, J. F. Wang, Z. Y. Huang, Y. He, A. Fischer and S. Cho, "Dicing Tape Format Die-Attach Film Selection Methodology for Ultra-Thin Stacked Die Chip Scale Packages", *Electronic Components and Technology Conference*, 2007.
2. X. J. Fan, I. Bekar, A. Fischer, Y. He, Z. Y. Huang, E. Prack, "Delamination/Cracking Mechanism Study for Ultra-thin Stacked-die Chip Scale Packages", *Intel Conference on Manufacturing Excellence (IMEC)*, San Diego, CA, 2006.
3. E. Prack and X. J. Fan, "Root Cause Mechanisms for Delamination/Cracking in Stack-die Chip Scale Packages", *International Symposium on Semiconductor Manufacturing (ISSM)*, September 25 - 27, Tokyo, Japan, 2006.
4. J. E. Galloway and B. M. Miles, "Moisture Absorption and Desorption Predictions for Plastic Ball Grid Array Packages", *InterSociety Conference on Thermal Phenomena*, pp. 180-186, 1996.
5. E. H. Wong, Y. C. Teo and T. B. Lim, "Moisture Diffusion and Vapor Pressure Modeling of IC Packaging", *Electronic Components and Technology Conference*, pp. 1372-1378, 1998.
6. G. Q. Zhang, W. D. van Driel and X. J. Fan, "Mechanics of Microelectronics", *Springer*, May 2006.
7. X. J. Fan, J. Zhou, G. Q. Zhang and L. J. Ernst, "A Micromechanics-Based Vapor Pressure Model in Electronic Packages", *ASME, Journal of Electronic Packaging*, Vol. 127, pp. 262-267, 2005.
8. X. J. Fan, G. Q. Zhang, W. V. Driel and L. J. Ernst, "Analytical Solution for Moisture-Induced Interface Delamination in Electronic Packaging", *Electronic Components and Technology Conference*, pp. 733-738, 2003.
9. X. J. Fan, G. Q. Zhang and L. J. Ernst, "Interfacial Delamination Mechanisms during Reflow with Moisture Preconditioning", *IEEE Transaction of Component, Manufacturing and Packaging Technology* (accepted)
10. N. Sun, D. C. Lin and D. G. Yang, "Finite Element Analysis of Hygro-Thermal Induced Failure in Plastic Packages", *International Conference on Electronics Packaging Technology*, pp. 381-385, 2003.
11. T. Y. Tee and Z. W. Zhong, "Integrated Vapor Pressure, Hygroswelling, and Thermo-Mechanical Stress Modeling of QFN Package during Reflow with Interfacial Fracture Mechanics Analysis", *Microelectronics Reliability*, 44, pp. 105-114, 2004.
12. P. Liu, L. Cheng and Y. W. Zhang, "Interface Delamination in Plastic IC Packages Induced by Thermal Loading and Vapor Pressure—A Micromechanics Model", *IEEE Transactions on Advanced Packaging*, Vol. 26, No. 1, pp. 1-9, 2003.
13. X. J. Fan and T. B. Lim, "Mechanism Analysis for Moisture-Induced Failure in IC Packages", *ASME International Mechanical Engineering Congress & Exposition, 11th Symposium on Mechanics of Surface Mount Assemblies*, pp. 1-12, 1999.
14. T. F. Guo and L. Cheng, "Modeling Vapor Pressure Effects on Void Rupture and Crack Growth Resistance", *Acta Materialia*, 50, pp. 3487-3500, 2002.
15. Y. He and X. J. Fan, "In-situ Characterization of Moisture Absorption, Desorption, and Diffusion in a Thin BT Core Substrate", *Electronic Components and Technology Conference*, 2007.